PLOS ONE

Transthyretin Is a Key Regulator of Myoblast Differentiation

Eun Ju Lee[1,9], Abdul R. Bhat[1,9], Majid Rasool Kamli[1], Smritee Pokharel[1], Tahoon Chun[2], Yong-Ho Lee[3], Sang-Seop Nahm[4], Joo Hyun Nam[5], Seong Koo Hong[6], Bohsuk Yang[6], Ki Young Chung[6], Sang Hoon Kim[7], Inho Choi[1]*

1 School of Biotechnology, Yeungnam University, Gyeongsan, Republic of Korea, 2 College of Life Sciences and Biotechnology, Korea University, Seoul, Republic of Korea, 3 Department of Biomedical Science, Catholic University of Daegu, Gyeongsan, Republic of Korea, 4 College of Veterinary Medicine, Konkuk University, Seoul, Republic of Korea, 5 Department of Physiology, Dongguk University, College of Medicine, Gyeongju, Republic of Korea, 6 Hanwoo Experiment Station, National Institute of Animal Science, RDA, Pyongchang, Republic of Korea, 7 Department of Biology, Kyung Hee University, Seoul, Republic of Korea

Abstract

Transthyretin (*TTR*) is a known carrier protein for thyroxine (T_4) and retinol-binding protein in the blood that is primarily synthesized in the liver and choroid plexus of the brain. Herein, we report that the *TTR* gene is expressed in skeletal muscle tissue and up-regulated during myotube formation in C2C12 cells. *TTR* silencing (TTR_{kd}) significantly reduced myogenin expression and myotube formation, whereas myogenin silencing ($MYOG_{kd}$) did not have any effect on *TTR* gene expression. Both TTR_{kd} and $MYOG_{kd}$ led to a decrease in calcium channel related genes including *Cav1.1*, *STIM1* and *Orai1*. A significant decrease in intracellular T_4 uptake during myogenesis was observed in TTR_{kd} cells. Taken together, the results of this study suggest that *TTR* initiates myoblast differentiation via affecting expression of the genes involved during early stage of myogenesis and the genes related to calcium channel.

Competing Interests: The authors have declared that no competing interests exist.

* E-mail: inhochoi@ynu.ac.kr

⑨ These authors contributed equally to this work.

Introduction

Myogenesis is the formation of multinucleated myofiber with a contractile capacity from muscle satellite cells (MSCs). Myogenesis involves cell cycle arrest, myogenic activation, cell alignment, multiple rounds of cell fusion and an increase in size with peripheral localization of the nuclei [1]. This process is highly regulated and involves growth factors, cytoskeletal proteins, and muscle specific transcription factors such as *myogenin* (*MYOG*) and *myocyte enhancer factor-2* (*MEF2*) which are regulated by an increase in cytosolic Ca^{2+} concentration [2], [3],[4], [5], [6].

Increased intracellular calcium activates intracellular protease, calpains, calcineurine and serine-threonine phosphatase, which plays a critical role in cell migration and fusion to myotube formation [7], [8], [9], [10]. Kubo Y. [11] proposed that T-type voltage-gated calcium channel (VGCC) and inward rectifier K^+ current increase the basal intracellular Ca^{2+} level, which may be essential to the initial stages of mesodermal stem cell differentiation. Ca^{2+} through T-type VGCC also contributes to other differentiation processes including neural differentiation [12] and neuroendocrine differentiation of prostate cancer cells [13]. Moreover, there is a great deal of evidence that Ca^{2+} influx through T-type VGCCs results in signalling that affects the expression of genes involved in cell proliferation, programmed cell death, and neuronal differentiation [14], [15], [16], [17], [18],

[19], [20]. Similarly, L-type VGCC like *Cav1.1* is also present in skeletal muscle [21]. In addition to VGCC, human myoblasts can generate Ca^{2+} signals by Ca^{2+} release from inositol 1,4,5-triphosphate-sensitive Ca^{2+} stores followed by entry through store operated calcium (SOCE) channels [3]. *STIM1* and *Orai1* are essential component of store-operated Ca^{2+} entry (SOCE) that is evoked in response to a fall in Ca^{2+} in the endoplasmic reticulum. *STIM1* is a calcium sensor in endoplasmic reticulum and *Orai1* in the plasma membrane [22], [23].

Transthyretin (*TTR*), which exists in tetrameric form is a carrier protein for thyroxine (T_4) and retinol-binding protein in the blood [24], [25], [26]. The liver and choroid plexus of the brain are major organs responsible for the synthesis of *TTR* in plasma and cerebrospinal fluid, respectively. In addition to the liver and brain, mRNA expression of *TTR* has been reported in the skeletal muscle of rats [27]. *TTR* gene knock-out mice increased neuropeptide Y, suggesting that *TTR* is critical in nervous system [28]. RNA interference targeting *TTR* in mammalian cells has been found to increase the initial efficacy of neural prosthetic devices before insertion [29]. We recently reported that *TTR* is induced in bovine primary MSC differentiation [30]. Herein, we investigated the role of *TTR* during myogenesis in C2C12. Silencing of *TTR* demonstrated the inability of cell alignment before fusion, leading to the formation of impaired myotubes.

Materials and Methods

Mouse Tissues

In this study, 6 or 18 weeks old male C57BL/6 mice were used for RNA isolation. Briefly, four week old mice were obtained from Daehan Biolink (Eumseong, Korea) and housed four per cage in a temperature-controlled room with a 12 hr light/12 hr darkness cycle. Throughout the study period, animals were allowed free access to standard rodent chow containing 4.0% (wt/wt) total fat (Rodent NIH-31 Open Formula Auto, Zeigler Bros., Inc., Gardners, PA, USA) and water. At 6 and 18 weeks of age, mice were anesthetized with sodium pentobarbital and exsanguinated. Tissue samples were then collected, quickly frozen in liquid nitrogen, and stored at $-80°C$ until processed for RNA extraction. For immunohistochemistry, mice were anesthetized by intraperitoneal injection of tribromoethanol (Avertin, 250 mg/kg, Sigma Aldrich CA, USA) for transcardial perfusion with PBS (phosphate buffered saline) to remove the blood. The animals were then perfusion fixed with 10% neutral buffered formalin, after which solid organs and skeletal muscles from the trunk and extremities were removed and post-fixed in the same fixative overnight at 4°C. The fixed organs were then processed for routine paraffin embedding, and the paraffin-embedded tissue blocks were cut to 6-μm thick sections for immunohistochemistry. The experimental protocols for the care and use of laboratory animals were approved by the Institutional Animal Care and Use Committee of Konkuk University.

Cell Culture

C2C12 cells, a murine myoblast cell line, were cultured in DMEM (Dulbecco's modified Eagle's medium; HyClone Laboratories, Logan, UT) supplemented with 10% FBS (fetal bovine serum, HyClone Laboratories) and 1% penicillin/streptomycin (Invitrogen, Carlsbad, CA, USA) at 37°C with 5% CO_2. For differentiation, cells grown to 70% confluence were switched to differentiation media (DMEM with 2% FBS) and then cultured for 0, 2, 4, and 6 days, during which time the medium was changed every two days. Cells were treated with T4 (50 ng/ml) for 4 and 6 days. C2C12 cells were kindly provided by Korean Cell Line Bank, Republic of Korea.

TTR and *MYOG* Knock-down

C2C12 cells grown in 6-well plates to 30% confluence were transfected with 1 ng of vector, *TTR* and *MYOG* shRNA construct per well using transfection reagent and transfection medium (Santa Cruz Biotechnology, CA, USA). After 3 days, the cells were treated with 2 μg/mL Puromyocin (Santa Cruz Biotechnology) for selection. Selected cells were grown upto 70% confluence before switching to differentiation media. Sequences of shRNA constructs are provided in Table S1.

Fusion Index

Fusion index was analyzed as previously described [31], [32]. Cell nuclei were stained with Giemsa G250 (Sigma Aldrich) and pictures were captured randomly at three different spots. Further, the number of nuclei in myotubes and the total number of nuclei in cell were counted in each field. Fusion index was calculated as the percentage of total nuclei incorporated in myotubes vs. total number of nuclei.

RNA Extraction and Real Time RT-PCR Analysis

Total RNA was extracted from the cells and tissues using Trizol™ reagent (Invitrogen) according to the manufacturer's protocol and then stored in diethylpyrocarbonate-treated H_2O at $-80°C$ until used. One microgram of RNA in a reaction mixture with a total volume of 20 μl was primed with oligo $(dT)_{20}$ primers (Bioneer, Daejeon, Korea) and then reverse transcribed at 42°C for 50 min and 72°C for 15 min. Subsequently, 2 μl of cDNA product and 10 pmoles of each gene-specific primer were used to perform PCR, which was conducted using a 7500 real-time PCR system (Applied Biosystems, Foster City, CA, USA). Power SYBR® Green PCR Master Mix (Applied Biosystems) was used as the fluorescence source. Primers were designed with the Primer 3 software (http://frodo.wi.mit.edu) using the sequence information listed at the National Center for Biotechnology Information. The detailed information about primer sequences are provided as Table S2.

Immunocytochemistry

C2C12 cells grown in a covered glass-bottom dish were treated with differentiation medium and stained for *TTR, MYOG, Cav1.1,* and *Cav3.1* protein following 0, 2, 4 and 6 days of incubation. Briefly, cells were rinsed with PBS and fixed with 4% formaldehyde, after which they were permeabilized with 0.2% Triton X-100 (Sigma Aldrich). The cells were then incubated with primary antibody (rabbit polyclonal IgG *TTR* (1:50), mouse monoclonal IgG *MYOG* (1:50), mouse monoclonal IgG *Cav1.1* (1:50), and rabbit polyclonal IgG *Cav3.1* (1:50), Santa Cruz Biotechnology) at 4°C in a humid environment overnight. Secondary antibody (1:100; Alexa Fluor 488 goat anti-rabbit and goat anti-mouse SFX kit; Molecular Probes, Eugene, OR, USA) was then applied for 1 hr at room temperature. The samples were rinsed with PBS, after which the nuclei were counterstained with 4′ 6′-diamino-2-phenylindole (DAPI; Sigma-Aldrich). Pictures were taken using a fluorescent microscope equipped with a digital camera (Nikon). Detail information about clone names of monoclonal antibodies are provided as Table S1.

Western Blot Analysis

Cells treated with differentiation media and cultured for different time periods were subjected to Western blot analysis. Briefly, after incubation, cells were washed with ice-cold PBS and lysed in RIPA lysis buffer containing protease inhibitor cocktail (Thermo Scientific, NH, USA). Total protein was isolated by centrifugation of the lysate at 13000 rpm for 10 min at 4°C, after which the protein concentrations were determined by the Bradford method using protein assay dye solution [33]. Total protein (40 μg) heated at 90°C for 3 min with ß-mercaptoethanol (Sigma-Aldrich) was electrophoresed in 10% SDS-polyacrylamide gel and then transferred to PVDF membrane (Millipore, MA, USA). The blots were subsequently blocked with 5% skim milk in TBST for an hour and then incubated overnight with *TTR* (1:500), *MYOG* (1:1000) or *β-actin* antibody (1:2000) (Santa Cruz Biotechnology) diluted with 3% skim milk in TBS at 4°C. Blots were next washed in TBST and incubated with horseradish peroxidase conjugated secondary antibody for an hour at room temperature, after which they were washed as described above and developed using Super Signal West Pico Chemiluminescent Substrate (Thermo Scientific).

Patch-clamp Analysis

Cells were transferred into a bath mounted on the stage of an inverted fluorescence microscope (Ti-U; Nikon Instruments, Inc., Melville, NY, USA). The bath (approximately 0.20 mL) was superfused at 5 mL/min, and voltage clamp experiments were performed at room temperature (22°C–25°C). Patch pipettes with a free-tip resistance of approximately 2.5 MOhm were connected to the head stage of a patch-clamp amplifier (Axopatch 200B;

Molecular Devices, Inc., Sunnyvale, CA, USA). The pCLAMP software v.10.2 and Digidata 1440 (Molecular Devices, Inc.) were used to acquire data and apply command pulses. Whole-cell currents were recorded at 10 kHz and low-pass filtered at 5 kHz. Current traces were stored and analyzed using Clampfit v.10.2 and Origin v. 8.0 (Microcal Inc, Northampton, MA, USA). For comparison of whole-cell currents between cells, the current amplitudes were normalized to the membrane area measured by electrical capacitance. The maximum absolute value of the current obtained (in pA) was divided by the cell capacitance (in pF). The pipette solution for the whole-cell patch clamp contained 100 mM Cs-aspartate, 32 mM CsCl, 10 mM ethylene glycol-bis (2-aminoethylether)-N,N,N',N'-tetraacetic acid (EGTA), 5 mM Mg-ATP, and 10 mM HEPES at pH 7.2 (titrated with CsOH). The bath solution for whole-cell recording of the VGCC contained 120 mM NaCl, 5 mM CsCl, 10 mM TEA-Cl, 10 mM BaCl$_2$, 10 mM glucose, 0.5 mM MgCl$_2$, and 10 mM HEPES at pH 7.4 (titrated with NaOH).

ELISA

Cell lysates extracted from cells differentiated for different lengths of time were used for ELISA to measure the T$_4$ concentration (DRG International, Inc. Margurg, Germany). Cell lysate and enzyme conjugate were added in a specific antibody-coated microtiter and then incubated for 1 hr at room temperature. The mixture was subsequently removed and washed to remove the unbound samples. After addition of the substrate solution for 20 min, the reaction was terminated by adding stop solution and the color intensity was measured using a spectrophotometer at 450 nm (Tecan Group Ltd. Switzerland).

Immunohistochemistry

TTR expression in mouse tissues was evaluated by immunohistochemistry using a *TTR* antibody (Santa Cruz Biotechnology). Briefly, paraffin-embedded tissue sections were deparaffinized, hydrated, and then quenched for endogenous peroxidase activity. The sections were blocked with 5% goat serum in PBS, after which they were incubated with the *TTR* antibody (2 μg/mL, Santa Cruz Biotechnology) overnight at 4°C. The sections were incubated with biotinylated anti-goat IgG (Vector, CA, USA) and subsequently with horseradish peroxidase-conjugated streptavidin (Vector). Positive signals were visualized by adding diaminobenzidine and hydrogen peroxide as substrates. A negative control experiment was also carried out by omitting the primary antibody. Stained sections were counterstained with methyl green and then dehydrated, mounted, and examined using a light microscope.

Statistical Analysis

The normalized expression means were compared using Tukey's Studentized Range (HSD) to identify significant differences in gene expression. A nominal p-value of less than 0.05 was considered to be statistically significant. Real time RT-PCR data were analyzed by one-way ANOVA using PROC GLM in SAS package ver. 9.0 (SAS Institute, Cary, NC, USA).

Results

TTR Expression and Localization in Mouse Tissues

TTR mRNA expression was observed in liver, muscle and brain tissues of different aged mice. The mRNA expression of the *TTR* gene was higher in 18 week old mice than 6 week old mice in muscle and liver tissues, with higher values being observed in liver tissue. The myogenesis marker genes, *MYOG* and *MYL2* (*Myosin*

light chain 2), being marker genes were expressed in higher levels and at earlier stages in muscle tissues. Moreover, *Cav1.1*, *STIM1* (*Stromal interaction molecule 1*) and *Orai* (*Calcium release-activated calcium channel protein 1*) were found to be highly expressed in muscle tissues (Fig. 1A). All the skeletal muscles stained for *TTR*, including forelimb, hind limb and trunk muscles, showed higher levels of *TTR* expression (Fig. 1B). Although the *TTR* expression was observed within the cytoplasm, but the intensity was not even throughout the muscle fibers.

TTR is Expressed during Myoblast Differentiation

To investigate the role of *TTR* during C2C12 myoblast differentiation into myotubes, cells were cultured and differentiated at different time points, after which their mRNA expression was analyzed by real time RT-PCR. The data after normalization revealed a more than 4 fold increase in the expression level of *TTR* at day 2, which remained almost constant to day 6 (Fig. 2A). The expression level of proteins was verified by Western blot and immunostaining (Fig. 2B, 2C). The cells were confirmed to be in the stage of myotube formation by checking the mRNA and protein expression of *MYOG* at different time points during cell differentiation (Fig. 2D, 2E, 2F).

TTR Knock-down Affects Myotube Formation

To assess the previously unrecognized role of *TTR* during myogenesis, cells were transfected either with 1 ng of *TTR* shRNA (TTR$_{kd}$) or vector GFP *(*TTR$_{wd}$). As shown in Fig. 3A, TTR$_{kd}$ significantly reduced mRNA expression of the genes involved in myogenesis at terminal differentiating stages, such as *MYOG* and *MYL2*. *Myf5* and *MyoD*, which are known to be involved in earlier stages of myogenesis, were unaffected at day 4. However, expression of *MyoD* was reduced significantly upto 75% when checked at day 2 (Fig. S1). shRNA transfection against *TTR* prevented the formation of myotubes as well as the decrease in the cytoplasmic distribution pattern of *TTR* and nuclear expression of *MYOG* protein (Fig. 3B, 3C: inset). The expression pattern obtained using immunoblot showed decreased levels of protein in TTR$_{kd}$ cells (Fig. 3D). Fusion index calculated at day 4 after TTR$_{kd}$ also agrees with the above observation, showing approximately 50% reduction as compared to TTR$_{wd}$ (Fig. 3E). In contrast, *MYOG* knock-down during differentiation did not have any effect on *TTR* mRNA expression (Fig. 3F). *MYOG* knock-down was also verified at the protein level by immunostaning and immunoblot analysis (Fig. 3G, 3H).

Voltage-gated Calcium Currents and Calcium-dependent Gene Expression

Calcium plays a critical role in multiple steps associated with myotube formation. In this study, to identify the functional expression of voltage-dependent Ca^{2+} channels (VDCCs) during myogenesis, the whole-cell patch-clamp recording of C2C12 cells at different time intervals was performed. Small T-type Ca^{2+} currents were detected in control cells at day 0 (Fig. 4A). However, only ~54% of the cells expressed measurable T-type Ca^{2+} currents. After five days of differentiation, in addition to T-type current, a distinct L-type Ca^{2+} current was detected (Fig. 4B) in response to 500 ms depolarizing pulses from a holding potential of -80 mV. Fig. 4B shows representative currents recorded at -30 mV (red line), where the T-type current shows the maximum curve (black arrow), and at 10 mV (blue line) where the L-type current shows a peak current amplitude (red arrow). Fig. 4C and 4D are the individual graphs obtained from the superimposed L/T type calcium currents data (Fig. 4B). Fig. 4C shows average

A.
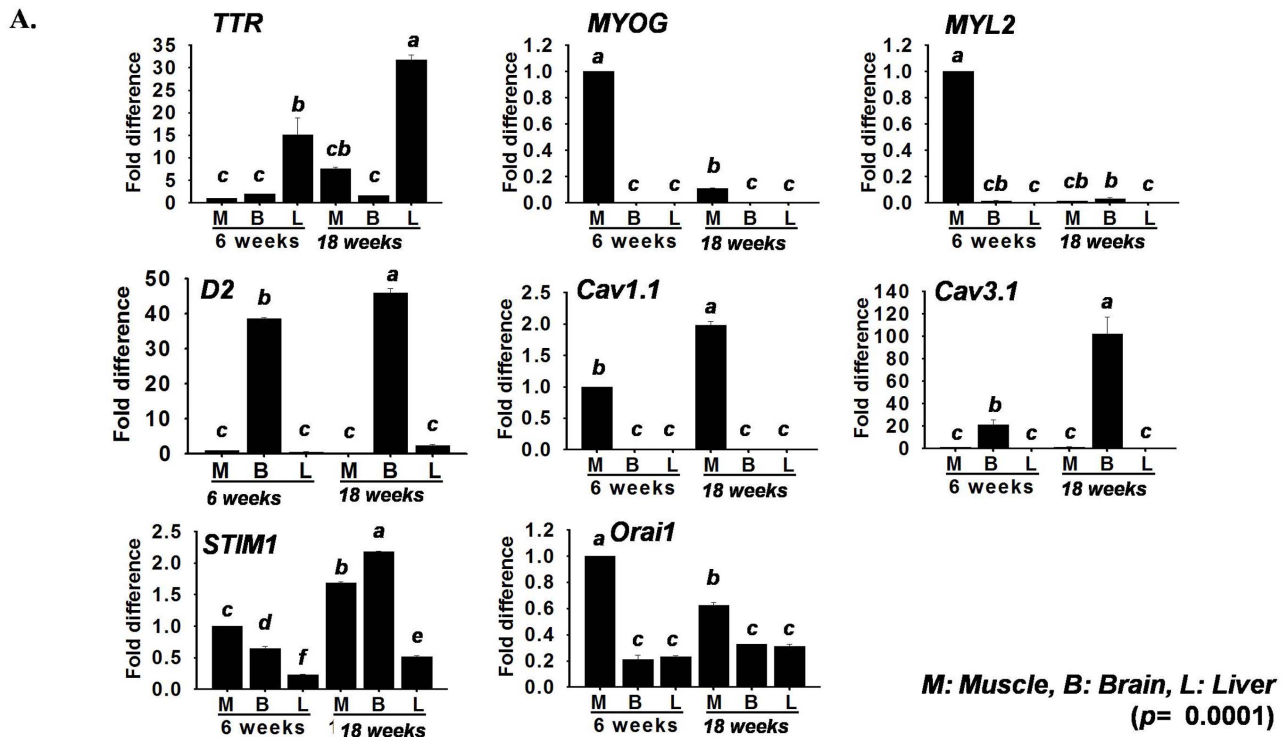
B.

Figure 1. *TTR* gene expression in different mouse tissues. A) mRNA expression showed in three different tissues, M (muscle), B (brain) and L (liver), by real time RT-PCR. *TTR, STIM1* and *Orai1* were found to be expressed in all tissues, while expression of *MYOG, MYL2, D2* (*Deiodinase 2*), *Cav1.1* and *Cav3.1* genes was specific to individual organs. B) *TTR* protein detection by immunohistochemistry revealed its presence in skeletal muscles of the forelimb, hind limb and trunk, as well as in the liver. The liver was used as a positive control (n = 3). The *p* value indicates the statistical significance of the data and different letters indicate significant difference among groups.
doi:10.1371/journal.pone.0063627.g001

current − voltage (I–V) relationship for the initial peak Ca^{2+} current in T-type channel (black arrow) at different day of culture. Fig. 4D shows an average I–V relationship for the secondary peak Ca^{2+} current in L-type channel (red arrow) at different day. Mixed T- and L-type currents were recorded over the −30 mV depolarizing pulse from a holding potential. After day 2, the T-type Ca^{2+} current was detected in most of the control cells (∼86%), whereas the L-type Ca^{2+} current was detected in ∼45% of C2C12 cells. The maximum detection rate (100%) of the T-type Ca^{2+} current was attained at day 3 (Fig. 4E). The detection probability of the L-type Ca^{2+} current gradually increased during myogenesis, reaching its maximum at day 5 (Fig. 4 E). Current density through T- and L-type Ca^{2+} channels increased significantly during myogenesis (Fig. 4F, P<0.05). Although the detection probability of the T- and L-type Ca^{2+} current gradually increased during myogenesis, the T- and L-type Ca^{2+} current densities did not show a gradual increase (Fig. 4C, 4D). The size of the myotubes was significantly higher in older cultures; however,

the current densities of each type of channel showed a transient increase at a specific point and increased only slightly during myogenesis. These electrophysiological data indicate that both T- and L-type Ca^{2+} channels are functionally expressed in differentiating C2C12 cells.

Cav1.1, Cav3.1 and *Orai1* mRNA showed a gradual increase in expression up to day 4 (Fig. 4G). In contrast, *STIM1* peaked at day 2. Localization of protein by immunostaining revealed a similar expression pattern (Fig. 4H). Moreover, the L-type calcium channel was blocked with nifedipine (100 μM) for 4 days during myogenesis and considerable reduction in myotube formation was observed (Fig. 4I). *Cav1.1* and *MYOG* mRNAs expression were significantly reduced by blocker, while *TTR* was unaffected (Fig. 4J).

TTR Controls the Calcium Channel

It was essential to identify the elements responsible for increased expression rates of T- and L-type Ca^{2+} channels during
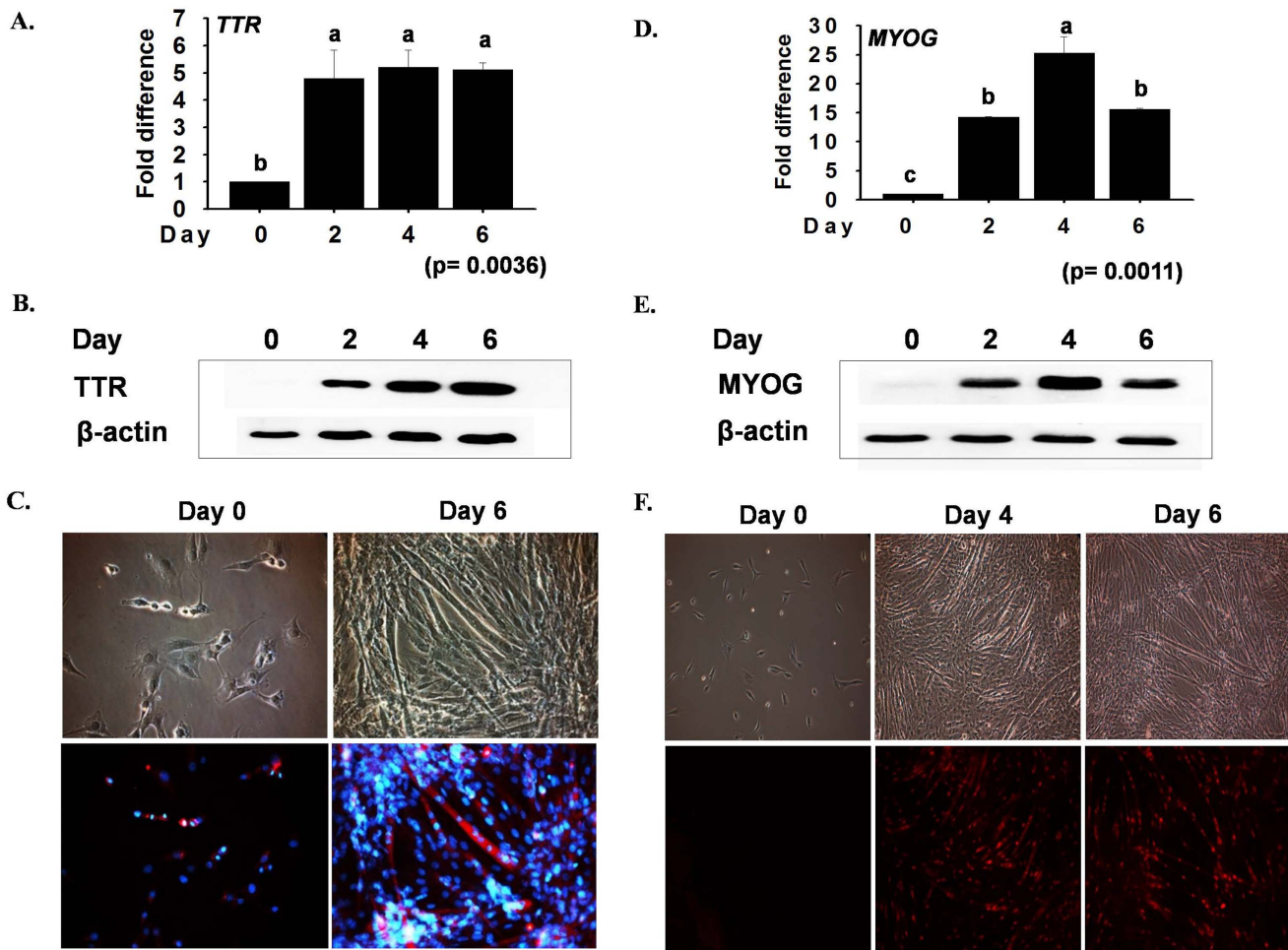
Figure 2. *TTR* and *MYOG* in C2C12 differentiation. C2C12 cells grown to 70% confluence and serum starved for 2, 4 and 6 days were used for mRNA and protein expression analysis. A) *TTR* mRNA showed up to a 5 fold difference in expression at day 2–6 upon real time RT-PCR analysis. B) Immunoblot analysis of *TTR* and ß-actin expression revealed low initial protein expression followed by a gradual increase with time. C) Distribution of *TTR* expression in cell cytoplasm as observed by immunostaining. The expression level was significantly upregulated at day 6. D) Time course study of mRNA expression of *MYOG* by real time RT-PCR. The maximum expression level was observed on day 4 of differentiation. E) Total proteins extracted from cells at different time points revealed very low expression of *MYOG* at the basal level that gradually increased up to day 4, then decreased at day 6. F) Cells differentiated and stained against the antibody of *MYOG* displayed the highest nuclear staining on day 4. The *p* value indicates the statistical significance of the data and different letters indicate significant difference among groups.
doi:10.1371/journal.pone.0063627.g002

myogenesis and confirm if there was any relationship between the *TTR* and VGCCs. No specific pharmacological blocker of *TTR* was available at the time of the study; therefore, *TTR*-specific shRNA was transfected into C2C12 cells. The prevention of the regulation of these Ca^{2+} channels was validated by the whole-cell patch-clamp recordings (Fig. 5A, 5B). As shown in Fig. 5C, the detection probability of T- and L-type Ca^{2+} channels was significantly reduced by TTR_{kd} at four days after switching to the differentiation medium. The current density between TTR_{wd} and TTR_{kd} cells was compared among cells expressing T- and L-type Ca^{2+} channels. In the case of TTR_{kd} cells, a significant decrease in detection probability and the current density was observed (Fig. 5D).

The mRNA expression of T- and L-type Ca^{2+} channel subunits (Fig. 5E) along with the *STIM1* and *Orai1* was found to be highly influenced by *TTR* silencing. The reduction in expression of *Cav1.1* in TTR_{kd} cells, demonstrating its direct involvement in myogenesis. In addition, *MYOG* silencing was also found to affect

Ca^{2+} entry related genes such as *STIM1, Orai1 and Cav1.1* (Fig. 5F), indicating that *MYOG* regulates these genes.

Cell Differentiation is also Affected by T_4

Thyroxin (T_4) is an important constituent of FBS used in cell culture experiments. In this study, the effect of T_4 on the expression of genes involved in myogenesis was investigated. *TTR* and *Cav1.1* expression were enhanced by T_4 treatment, while this effect was small in other genes (Fig. 6A). In wild type cells (TTR_{wd}), wider myotube formation was observed after T_4 treatment. However, there was no apparent change in the morphology of TTR_{kd} cells with or without T_4 treatment (Fig. 6B). Changes in the T_4 concentration of cells were measured by ELISA (Fig. 6C). A gradual increase in T_4 concentration was observed in TTR_{kd} cells. In contrast, the concentration of T_4 in TTR_{wd} cells increased up to day 4 and then decreased at day 6. Interestingly, the intracellular T_4 concentration of TTR_{wd} cells was significantly higher than that of TTR_{kd} cells at day 4, when C2C12 cells showed peak myotube formation. The increase in
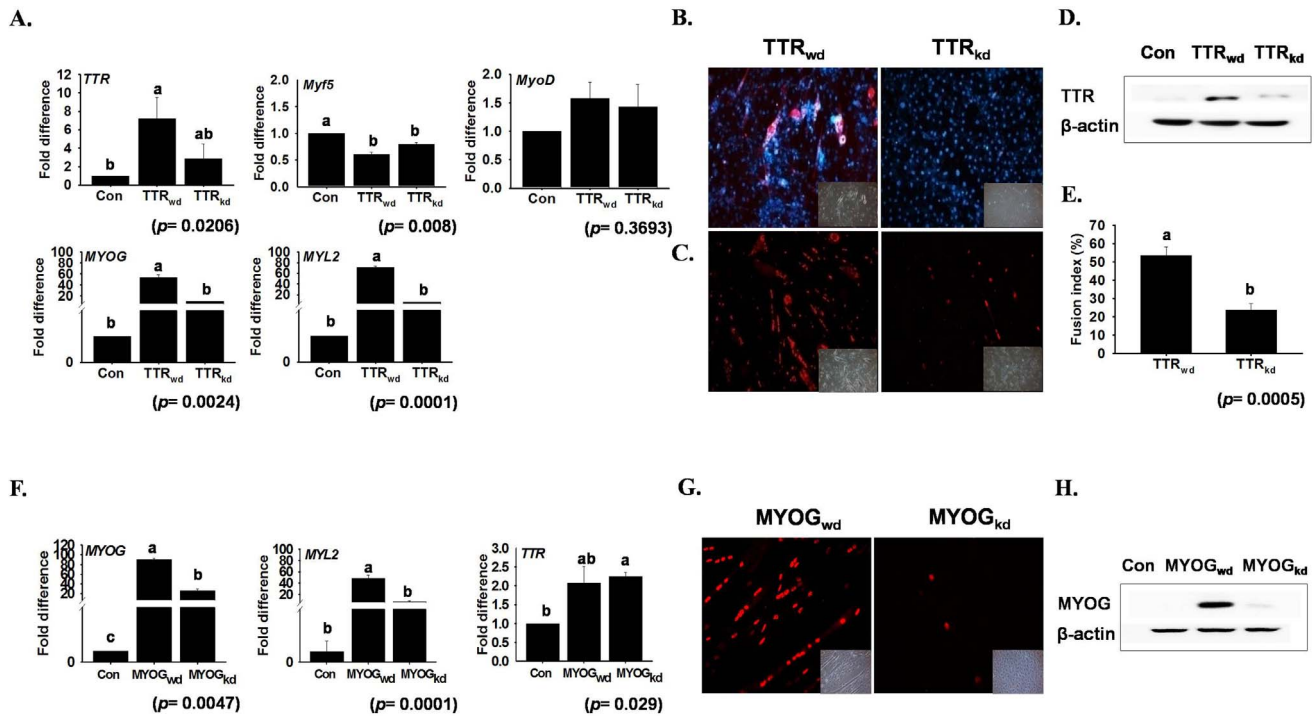
Figure 3. *TTR* and *MYOG* knockdown and their effect. TTR knock-down cells (TTR$_{kd}$) showed altered mRNA expression of myogenic genes. A) A decrease in mRNA expression was observed on day 6 of transfection in *TTR* and day 5 in *MYOG* and *MYL2*. However *Myf5* and *MyoD* showed little enhancement. Control indicates the time at which cells were transfected (n = 3). B) Immunostaining of cells transfected with either TTR$_{wd}$ or TTR$_{kd}$ (day 6). A significant decrease of cytoplasmic *TTR* protein was observed in TTR$_{kd}$ cells when compared with TTR$_{wd}$ cells. C) Similarly, TTR$_{kd}$ led to decreased nuclear myogenin protein expression. D) Western blot of TTR$_{kd}$ agrees with the immunostaining results. E) Fusion index was performed with TTR$_{wd}$ and TTR$_{kd}$ at day 4. A significant decrease of nuclei fusion in TTR$_{kd}$ was analyzed as compared to TTR$_{wd}$ cells. F) mRNA expression of *MYOG* knock-down in C2C12 and its effect on *MYL2* and *TTR*, which peaked on day 4 of differentiation. *MYL2* is affected by *MYOG* knock-down, while *TTR* showed no change. G &H) immunostaining and immunoblot analysis verifying myogenin knockdown up to the protein level during differentiation at day 4. The *p* value indicates the statistical significance of the data and different letters indicate significant difference among groups.
doi:10.1371/journal.pone.0063627.g003

intracellular T$_4$ concentration can be assumed to be due to the presence of T$_4$ in cell culture media and its transport across the membrane.

Discussion

TTR-interaction during Myoblast Differentiation

TTR, which is known as a carrier protein for thyroxin and retinol binding protein, has been shown to play a critical role in homeostasis of the nervous system [34]. We previously identified *TTR* as one of the genes highly up-regulated in different depots of bovine muscle tissue during myogenesis [30]. This was a novel finding, as the protein had previously been reported as a systematic precursor to deposition and amyloid fiber formation. Immunohistochemical analysis was used to detect the presence of *TTR* protein in skeletal muscles of the forelimb, hind limb and trunk, as well as in the liver (control). The presence was further confirmed by mRNA expression of *TTR* in different muscle depots (Fig. 1). This study describes the role of *TTR* as a key factor in myoblast differentiation. In this study, shRNA that silenced *TTR*, was used to investigate (i) inhibition of myotube formation based on *MYOG* and *MYL2* mRNA expression (ii) changes in mRNA expression of the calcium channel related genes, *STIM1*, *Orai1*, *Cav1.1* and *Cav3.1*, and (iii) time dependent occurrence of voltage-gated calcium currents during myogenesis. Our results are in accordance with Mock et al [35], in which they demonstrate the decrease in muscle mass of a *TTR* null mouse.

To investigate the function of *TTR* in myogenesis, C2C12 cells were transfected with shRNA against *TTR* and observed for changes in cell morphology and gene expression. Microscopic observations revealed a reduction in myotube formation in *TTR* silenced cells when compared with wild type (wd) cells. These findings were supported by decrease in *TTR* mRNA and protein expression observed by real time RT-PCR and immunostaining, respectively. Muscle differentiation is accompanied by specific alterations in the pattern of muscle specific gene expressions [36], particularly those of two groups of transcription factors, the *MyoD* family (including *Myf5*, *MyoD*, *MYOG*) and the *MEF2* family. To confirm this, the mRNA expression of these genes was compared in TTR$_{kd}$ and TTR$_{wd}$ cells. *Myf5* was unaltered, whereas variation in the expression of *MYOD*, *MYOG* and *MYL2* was observed. *Myf5* and *MyoD* are known to exist in the early stages of myoblast differentiation [37], while *MYOG* is expressed throughout myotube formation and *MYL2* is expressed at a later stage. As shown in Fig. 2 and 3, *TTR* silencing affects the expression of *MYOG*, which can be assumed to be a result of the early interference of *TTR* during myogenesis. The effect of *TTR* on *MYL2* also confirms its interference during myogenesis. The time course study revealed that the expression of *MYOG* and *MYL2* was highest on day 4, after the culture medium was replaced with differentiation medium. To confirm the role of *TTR* in myogenesis via involvement of the calcium channel(s), the mRNA expression of *STIM1*, *Orai1*, and VGCCs was studied in detail. Darbelly et al. [38] reported that *STIM1* and *Orai1*-dependent store operated
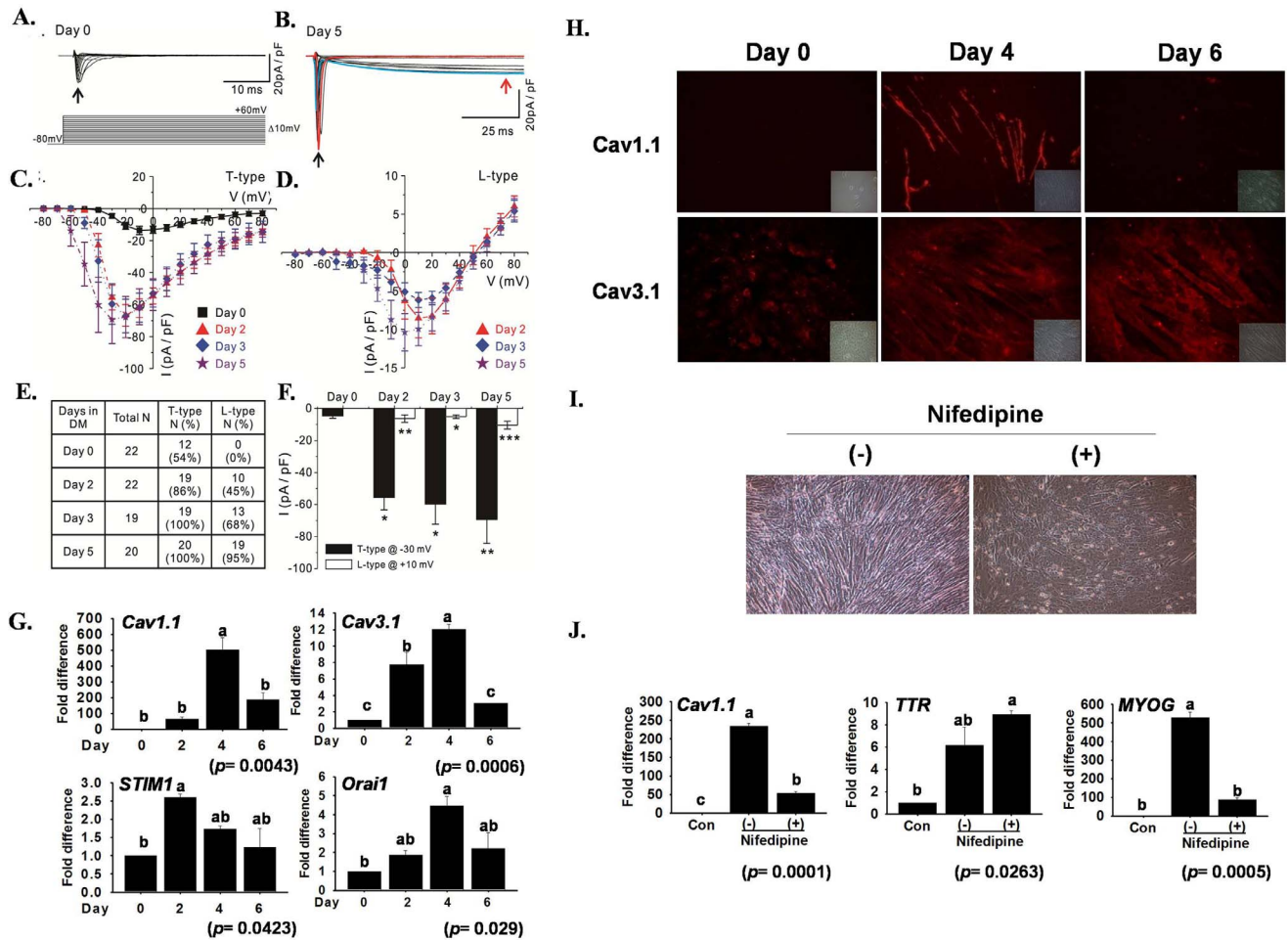
Figure 4. L-type and T-type calcium current and expression of Ca^{2+} channel related genes during myogenesis. Whole-cell patch clamp recordings in response to 500 ms depolarization from a holding potential (HP) of −80 mV stepped to values between −80 mV and 90 mV for 500 ms. Ba^{2+} (10 mM) was used as a charge carrier. A) Superimposition of different traces under the control conditions in response to test pulses from −80 to 40 mV. B) Representative superimposed L/T-type Ca^{2+} current traces after 5 days of culture in differentiation medium (DM). C) Average current − voltage (I–V) relationship for the initial peak Ca^{2+} current (T-type, black arrow) at 0 (n = 12), 2 (n = 19), 3 (n = 19), and 5 (n = 20) days after culture in DM. D) Average I–V relationship for the secondary peak Ca^{2+} current (L-type, red arrow) at 2 (n = 10), 3 (n = 13), and 5 (n = 19) days after culture in DM. E) Summary of the detection probabilities of L/T-type Ca^{2+} current from the patch clamp recording after culture in DM. Note that both the T- and L-type detection rate gradually increases through the time course. F) Histograms of the current density of the T-type calcium current (measured using a test pulse at −30 mV, HP −80 mV) and the L-type (measured at 0 mV). mRNA expression of Ca^{2+} channel related genes was analyzed by real-time RT-PCR. G) Up-regulated mRNA expression of calcium channel related genes during myogenesis at different time points. *Cav1.1* (L-type), *Cav3.1* (T-type) and *Orai1* showed maximum expression on day 4, whereas *STIM1* on day 2 represents the variation in calcium homeostasis at given time intervals. H) Immunofluorescence labeling indicates the distribution of *Cav1.1* and *Cav3.1* protein in the cytoplasm on days 0, 4 and 6. The highest expression of *Cav1.1* and *Cav3.1* protein was observed on day 4 and 6, respectively. I) Cells were treated with nifedipine as a L-type Ca^{2+} channel blocker (100 μM) during differentiation A change in morphology and decrease in myotube formation was observed. J) Effect of nifedipine on mRNA expression of *TTR*, *Cav1.1* and *MYOG*. Nifedipine reduced *Cav1.1* and *MYOG* expression, whereas *TTR* was unaffected (mean ± S.D., n = 3). The *p* value indicates the statistical significance of the data and different letters indicate significant difference among groups.
doi:10.1371/journal.pone.0063627.g004

calcium entry (SOCE) plays a crucial role in the regulation of myogenesis in human myoblasts. Specifically, they found a correlation between the amplitude of SOCE and *MYOG/MEF2* expression and reported that SOCE was the limiting factor in the signaling cascade that controls the fate of myoblasts. However, SOCE amplitude is regulated by *STIM1* and *Orai1*. In the time course study, *Orai1*, *Cav1.1*, and *Cav3.1* were found to be up-regulated, with their expression peaking at day 4. However, the expression of these genes was down-regulated in TTR$_{kd}$ cells when compared to TTR$_{wd}$ SOCE and VGCC calcium influx functions in reciprocal mechanism pathways. Nevertheless, excitable cells have been found to express SOCE proteins, but contribute little to

Ca^{2+} influx [39], [40], whereas non-excitable cells express VGCC proteins but lack voltage-gated Ca^{2+} currents [41], [42]. The decrease in mRNA expression of SOCE genes, namely *STIM1* and *Orai1*, and the mRNA expression of VGCC genes, namely *Cav1.1* and *Cav3.1*, draws attention to the crucial role played by *TTR* during myogenesis. These results suggest that *TTR* initiates myogenesis in both excitable and non-excitable cells.

Effect of *myogenin* Silencing

Most studies conducted to investigate the process of differentiation have focused on the expression of *MYOG*, a marker gene involved in myogenesis. In the present study, C2C12 cells were
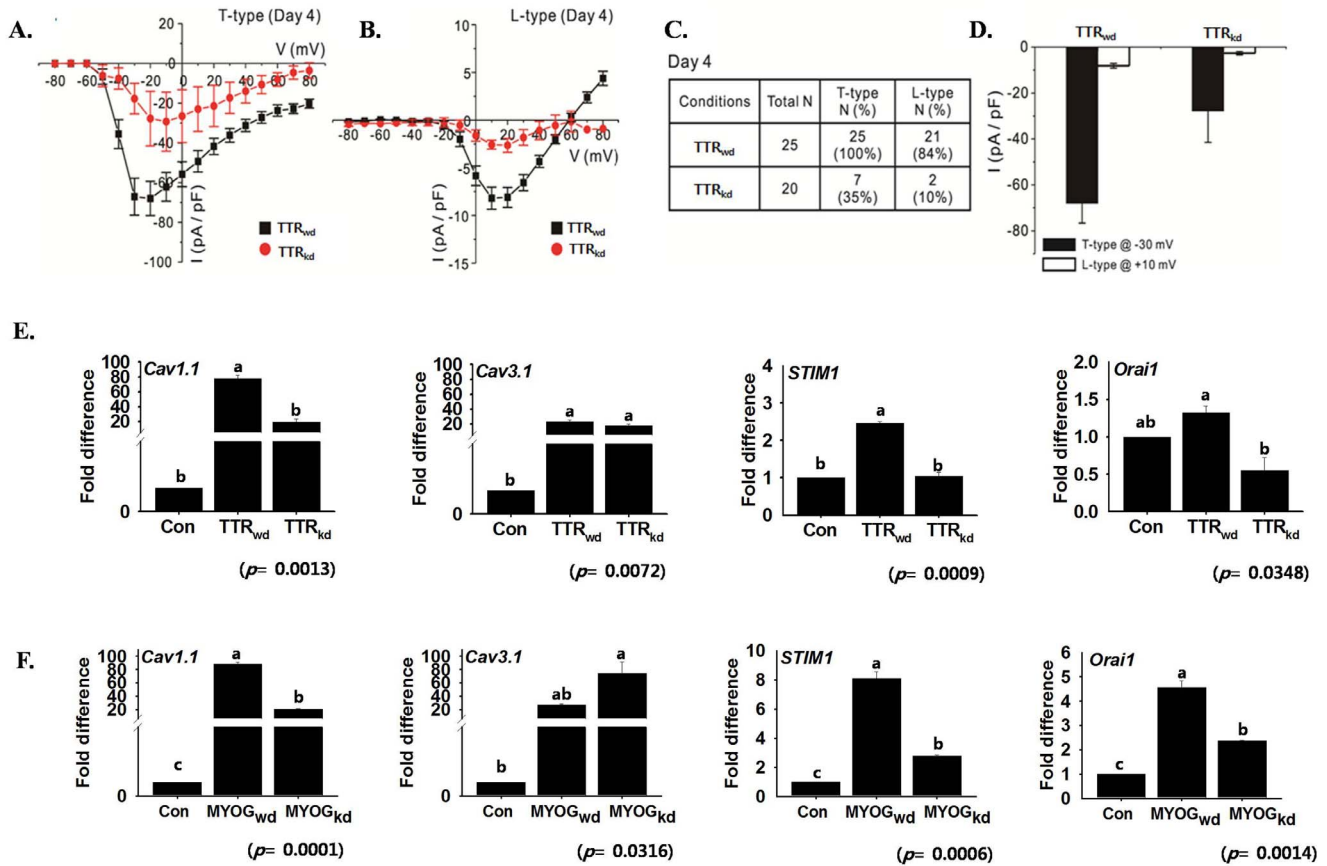
Figure 5. Effects of *TTR* silencing on voltage operated Ca²⁺ channels during the myogenesis. Currents were evoked by 500-ms step pulses in 10 mV increments applied from −80 mV HP (see voltage protocol in Figure 3). Current traces were obtained for every 10 mV step between −80 and 80 mV. A) I–V relationships for T-type Ca²⁺ current from TTR$_{wd}$ (n = 25) and TTR$_{kd}$ (n = 21). The magnitude of each current was measured on day 4 after culture in DM. B) I–V relationships for L-type Ca²⁺ current from TTR$_{wd}$ (n = 7) and TTR$_{kd}$ (n = 2). C) Summary of the detection probabilities of L/T-type Ca²⁺ current between TTR$_{wd}$ and TTR$_{kd}$ at day 4 after culture in DM. Note that the detection probability was significantly decreased in TTR$_{kd}$. D) Histograms of the current density of the T-type calcium current (measured using a test pulse at −30 mV, HP −80 mV) and the L-type (measured at 10 mV). E & F) mRNA expression assessed by real-time RT-PCR on *Cav1.1*, *Cav3.1*, *STIM1* and *Orai1* in TTR$_{wd}$, TTR$_{kd}$ or MYOG$_{kd}$ cells on day 4 of transfection. TTR knock-down resulted in a decreased effect on all calcium channel related genes. *MYOG* knock-down showed decreased expression of *Cav1.1*, *STIM1* and *Orai1*. Control indicates day 0 (mean ± S.D., n = 3). *p* value indicates the statistical significance of the data and different letters indicate significant difference among groups.
doi:10.1371/journal.pone.0063627.g005

transfected with shRNA against *MYOG* and an expected change in cell morphology and decrease in myotube formation was observed. While MYOG$_{wd}$ cells showed well-established myotubes, no myotubes were observed in the MYOG$_{kd}$ cells. mRNA analysis revealed a decrease in the expression of *MYOG* and *MYL2*; however, *TTR* remained almost unaffected, indicating that *TTR* may remain upstream of *MYOG* during differentiation. Surprisingly, real time RT-PCR analysis revealed a decrease in the mRNA expression of *STIM1*, *Orai1* and *Cav1.1*, while *Cav3.1* showed increased expression. These findings indicate that *MYOG* acts during the initial stage of myotube formation. While studying the ability of mononucleated myocytes to synthesize DNA during myogenesis, Andrés. [43] found that the induction of *MYOG* protein precedes that of p21. DNA synthesis revealed that *MYOG* is expressed in the premitotic state of myocytes and p21, a marker of the postmitotic state of myocytes. The decrease in expression of *STIM1*, *Orai1* and *Cav1.1* involved in myogenesis due to silencing of *MYOG* can be assumed to occur in conjunction with the early expression of *MYOG*. Immunocytochemical analysis revealed that less *MYOG* was present in the nuclei. However, real time RT-PCR

analysis revealed that *TTR* was unaffected, while *STIM1* and related genes were greatly influenced by *MYOG* silencing. It is speculated that: i) *TTR* is upstream to *MYOG* and ii) *MYOG* either directly (such as through gene regulation by attachment to the *STIM1* promoter) or indirectly (by some unknown pathway) induces the *STIM1* expression, which subsequently works through *Orai1* and/or iii) the early expression of *MYOG* had a direct effect on VGCCs to influence myotube formation. The expression of *TTR* and its silencing effect on *MYOG*, *STIM1*, *Orai1* and VGCC related genes suggests that *TTR* is the key regulator during myogenesis and activate the *MYOG* transcription factor through some unknown mechanism. However, a detailed investigation is needed to determine exactly how *TTR* affects *MYOG* and how *MYOG* silencing affects the mRNA expression of *STIM1*, *Orai1* and *Cav1.1*.

TTR Influences VGCCs

Calcium signaling plays an important role in many cellular processes including cell growth and differentiation, and Ca²⁺entry into skeletal muscle fiber has been known to contribute to calcium
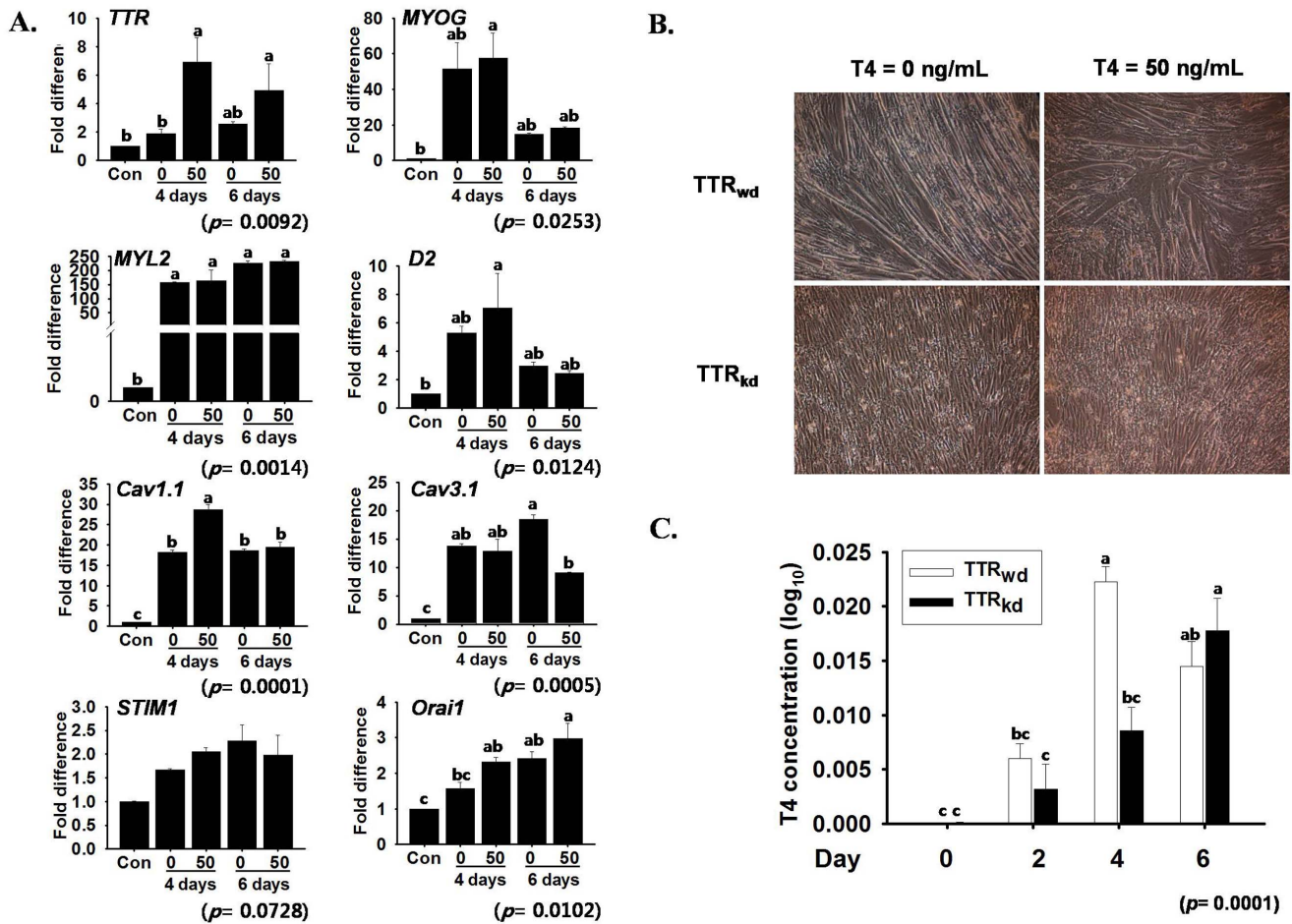
Figure 6. Thyroid hormone effect on myogenesis. A. mRNA expression of the *TTR* gene and genes associated with the calcium channel and myogenesis was assessed by real-time RT-PCR at day 4 and 6 of differentiation with 50 ng/mL T_4. *TTR* expression was greatly influenced by T_4 treatment; however, the expression of other genes related to myogenesis and the Ca^{2+} channel were variable. B) The T_4 effect on *TTR* silencing showed no change on day 6. C) T_4 concentration measured by ELISA in the extracts of TTR_{wd} and TTR_{kd} cells, respectively, at different days of differentiation. Control indicates the time at which proliferative media was replaced with differentiation medium. *p* value indicates the statistical significance of the data and different letters indicate significant difference among groups.
doi:10.1371/journal.pone.0063627.g006

signaling. It has been suggested that T-type calcium current ($I_{Ca,T}$) in developing muscles is involved in pacemaker-like activity while L-type calcium current ($I_{Ca,L}$) could serve as an early contraction triggering mechanism and/or initially to fill and maintain the intracellular calcium stores [44]. In this study, we revealed a role of VGCC during C2C12 cell differentiation. Using TTR_{kd}, we found that *TTR* regulates the amplitude of VGCC during C2C12 cell differentiation. The effect of TTR_{kd} was observed in all cells tested, regardless of the time spent in cultures. It has been reported that the *TTR*-induced increase in Ca^{2+} resulted exclusively from an influx of extracellular Ca^{2+} across the plasma membrane, mostly via L- and N-type VGCCs [45]. Also Ca^{2+} concentrations in myoblast cells upon treatment with the nifedipine, an L-type Ca^{2+} blocker has been found to inhibit the myogenic differentiation [46]. Mibefradil, a T- type Ca^{2+} blocker had been found responsible for 57% inhibition of cell fusion. However, mibefradil blocks $I_{K(DR)}$, $I_{(h-eag)}$, and $I_{K(IR)}$ in addition to $I_{ca(T)}$. Since it is known that blocking 50% of $I_{K(IR)}$ reduces cell fusion by only 25%, it was speculated that the 32% inhibition in cell fusion by mibefradil was either an isolated or combined effect of $I_{K(DR)}$, $I_{(h-eag)}$, or $I_{ca(T)}$ [47]. In the present study, $I_{ca(T)}$ was detected before the concentration of the serum was reduced. However, the detection

rate increased and reached 100% in fused cells at day 3. The $I_{Ca(L)}$ current was not detected in the early stage, but there was a drastic increase in cells with $I_{Ca(L)}$ on day 2, after which the myocytes started to fuse. A gradual increase in the detection rate was found thereafter. Chronic application of 100 µM of nifedipine, a concentration that fully inhibits $Ca_V1.1$, sharply affected the C2C12 myoblast fusion. RT-PCR experiments revealed that the expression of *Cav1.1* and *MYOG* decreased, while that of *TTR* remained unaffected. Repeating patch clamping experiments with cells transfected with vector (TTR_{wd}) and shRNA against *TTR* (TTR_{kd}) revealed a decrease in the detection rate of both T- and L-types in TTR_{kd}, indicating that *TTR* plays a clear role in initiation of and during the cell differentiation process. It has been reported that SOCE in skeletal muscle requires both *STIM1* and *Orai1*, and SOCE and VGCC represent two distinct and independent molecular entities [39]. However, in this study, the silencing of *TTR* and *MYOG* was found to lead to a decrease in both SOCE proteins (*STIM1* and *Orai1*) and *Cav1.1*. These results demonstrate the crucial role of *TTR* during myogenesis in both excitable (voltage-gated calcium entry) and non-excitable (store-operated calcium channel) cells. Accordingly, a detailed study is required to

understand this relationship of *TTR* with excitable and non-excitable cells.

Effect of Thyroid Hormones

Thyroid hormone (T_4) plays an important role in cellular development, differentiation and metabolism [48], [49], [50]. Specifically, T_4 regulates gene expression mediated through thyroid hormone receptors in the nucleus of target cells. *TTR* is one of the three primary T_4 transport proteins found in serum and has a high binding affinity for T_4 [51]. *TTR* can both inhibit and enhance T_4 transport across the membrane. To identify the effects of T_4 in *TTR* expression and myogenesis, the cells were cultured in differentiation medium supplemented with T_4 hormone. Based on the mRNA expression of different genes involved in myogenesis, *TTR* was highly expressed and showed a four fold difference in response to treatment with 50 ng/mL T_4. However, other genes related to myogenesis including *STIM1, Orai1* and *Cav3.1* showed almost no change in response to T_4 treatment. When cells transfected with shRNA against *TTR* (TTR_{kd}) and vector (TTR_{wd}) were treated with T_4, no enhancement of myotube formation in TTR_{kd} cells was observed, while TTR_{wd} cells treated with T_4 showed a slight increase in myotube size. Moreover, T_4 concentration analysis showed that the T_4 in cells was higher on day 4, at which the expression of most genes involved in myogenesis peaked. It could be attributed to the fact that the thyroid hormone is considered as positive regulator of muscle development [52]. This result indicates a direct or indirect role of *TTR* in uptaking T_4 during myogenesis.

In summary, our work demonstrates a robust inhibition of myoblast differentiation in response to *TTR* silencing in C2C12 cells. The findings presented herein indicate that *TTR* initiates cell differentiation either by influencing the early stage expression of the transcription factor *MYOG* or by directly influencing the SOCE proteins *STIM1 and Orai1* as well as the VGCC proteins *Cav1.1* and *Cav3.1*. The effects of *TTR* on two distinct calcium influx pathways indicate that *TTR* is an essential entity that initiates the process of myogenesis, regardless of whether the cells are excitable or non-excitable in terms of calcium influx.

Supporting Information

Figure S1   *MyoD* expression in *TTR* knock-down cells. A) Decreased cell alignment was seen in TTR knock-down cells (TTR_{kd}) as compared to *TTR* wild type cells (TTR_{wd}) on day two as seen under phage contrast microscope. B) TTR_{kd} showed reduced mRNA expression of both *TTR* and *MyoD* as compared to TTR_{wd} by real-time PCR on day 2 in C2C12 during myogenesis. p value indicates the statistical significance of data and different letters indicate significant difference among groups. (TIF)

Table S1   shRNA sequence information. The table shows a list of shRNA sequence information. (DOC)

Table S2   Primer information. The table shows a list of primer indicating species, gene names, product size, Tm (temperature), and primer sequences (F: forward, R: reverse). (DOC)

Table S3   Antibody information. The table shows a list of antibody used and its clone names. (DOC)

Acknowledgments

Author Contributions

Conceived and designed the experiments: IC EJL. Performed the experiments: EJL SP ARB JHN. Analyzed the data: EJL ARB JHN IC. Contributed reagents/materials/analysis tools: TC Y-HL S-SN SKH BY KYC SHK. Wrote the paper: ARB MRK SP IC EJL.

References

1. Chargé SB, Rudnicki MA (2004) Cellular and molecular regulation of muscle regeneration. Physiological Reviews 84: 209–238.
2. Pavlath GK (2010) Spatial and functional restriction of regulatory molecules during mammalian myoblast fusion. Experimental Cell Research 316: 3067–3072.
3. Arnaudeau S, Holzer N, Konig S, Bader CR, Bernheim L (2006) Calcium sources used by post-natal human myoblasts during initial differentiation J Cell Physiol 208: 435–445.
4. Konig S, Hinard V, Arnaudeau S, Holzer N, Potter G, et al. (2004) Membrane hyperpolarization triggers myogenin and myocyte enhancer factor-2 expression during human myoblast differentiation. J Biol Chem 279: 28187–28196.
5. Konig S, Beguet A, Bader CR, Bernheim L (2006) The calcineurin pathway links hyperpolarization (Kir2.1)-induced Ca2+ signals to human myoblast differentiation and fusion. Development 133: 3107–3114.
6. Le GF, Rudnicki MA (2007) Skeletal muscle satellite cells and adult myogenesis. Curr Opin Cell Biol 19: 628–633.
7. Barnoy S, Glaser T, Kosower NS (1997) Calpain and calpastatin in myoblast differentiation and fusion: effects of inhibitors. Biochim. Biophys Acta 1358: 181–188.
8. Friday BB, Mitchell PO, Kegley KM, Pavlath GK (2003) Calcineurin initiates skeletal muscle differentiation by activating MEF2 and MyoD. Differentiation 71: 217–227.
9. Pavlath GK, Horsley V (2003) Cell fusion in skeletal muscle central role of NFATC2 in regulating muscle cell size. Cell Cycle 2: 420–423.
10. O'Connor RS, Mills ST, Jones KA, Ho SN, Pavlath GK (2007) A combinatorial role for NFAT5 in both myoblast migration and differentiation during skeletal muscle myogenesis. J Cell Sci 120: 149–159.
11. Kubo Y (1991) Electrophysiological and immunohistochemical analysis of muscle differentiation in a mouse mesodermal stem cell line. J Physiol 443: 711–741.
12. Chemin J, Nargeot J, Lory P (2002) Neuronal T-type alpha1H calcium channels induce neuritogenesis and expression of high-voltage-activated calcium channels in the NG108–15cellline. J Neurosci. 22: 6856–6862.
13. Mariot P, Vanoverberghe K, Lalevee N, Rossier MF, Prevarskaya N (2002) Overexpression of an alpha 1H (Cav3.2) T-type calcium channel during neuroendocrine differentiation of human prostate cancer cells. J Biol Chem 29: 10824–33.
14. Spitzer NC, Gu X, Olson E (1994) Action potentials, calcium transients and the control of differentiation of excitable cells. Curr Opin Neurobiol 4: 70–77.
15. Bito H, Deisseroth K, Tsien RW (1997) Ca2+-dependent regulation in neuronal gene expression. Curr Opin Neurobiol 7: 419–429.
16. Nicotera P, Orrenius S (1998) The role of calcium in apoptosis. Cell Calcium 23: 173–80.
17. Marshall J, Dolan BM, Garcia EP, Sathe S, Tang X, et al. (2003) Calcium channel and NMDA receptor activities differentially regulate nuclear C/EBPbeta levels to control neuronal survival. Neuron 14: 625–39.
18. Weick JP, Groth RD, Isaksen AL, Mermelstein PG (2003) Interaction with PDZ proteins are required for L-type calcium channels to activate cAMP response element-binding protein-dependent gene expression. J Neurosci 23: 3446–3456.
19. Grassi C, D'Ascenzo M, Torsello A, Martinotti G, Wolf F, et al (2004) Effects of 50 Hz electromagnetic fields on voltagegated Ca2+ channels and their role in modulation of neuroendocrine cell proliferation and death. Cell Calcium 35: 307–315.
20. Toescu EC, Verkhratsky A, Landfield PW (2004) Ca2+ regulation and gene expression in normal brain aging. Trends Neurosci 27: 614–620.
21. Catterall WA (2011) Voltage-gated calcium channels. Cold Spring Harb Perspect Biol 3: a0003947.
22. Numaga TT, Putney JW (2012) Role of STIM1 and Orai1-mediated calcium J entry in Ca2+-induced epidermal keratinocyte differentiation. J Cell Sci doi: 10.1242/jcs.115980.
23. Baryshnikov SG, Pulina MV, Zulian A, Linde CI, Golovina VA (2009) Orai1, a critical component of store-operated Ca2+ entry, is functionally associated with Na+/Ca2+ exchanger and plasma membrane Ca2+ pump in proliferating human arterial myocytes. Am J Physiol Cell Physiol 297: C1103–11012.
24. Samantha JR (2007) Cell and Molecular Biology of Transthyretin and Thyroid Hormones. Int Rev Cytol 258: 137–193.

25. Johnson SM, Connelly S, Fearns C, Powers ET, Kelly JW (2012) The transthyretinamyloidoses: from delineating the molecular mechanism of aggregation linked to pathology to a regulatory-agency-approved drug. J Mol Biol 10: 185–203.

26. Hamiltona JA, Bensonb MD (2001) Transthyretin: a review from a structural perspective. CMLS, Cell. Mol Life Sci 58: 1491–1521.

27. Dianne RS, Joseph H, KennJeth S, Eric AS, DeWitt G (1985) Demonstration of Transthyretin mRNA in the Brain and other Extrahepatic Tissues in the Rat. J Biol Chem 260: 11793–11798.

28. Nunes AF, Liz MA, Franquinho F, Teixeira L, Sousa V, et al. (2010) Neuropeptide Y expression and function during osteoblast differentiation–insights from transthyretin knockout mice. FEBS J 277: 263–75.

29. Smith KL, Herron B, Dowell MN, Wu H, Kim SJ, W. etal. (2012) Knockdown of cortical transthyretinexpression around implanted neural prosthetic devices using intraventricular siRNA injection in the brain. J Neurosci Methods 203: 398–406.

30. Lee EJ, Lee HJ, Kamli MR, Pokharel S, Bhat AR, Lee YH, et al. (2012) Depot-specific gene expression profiles during differentiation and transdifferentiation of bovine muscle satellite cells, and differentiation of preadipocytes. Genomics 100: 195–202.

31. Brigitle P, Frederic D, Yves G (1998) Muscle Differentiation of Normal and Double-Muscled Bovine Foetal Myoblasts in Primary Culture. Basic Appl Myol 8: 197–203.

32. Veliça P, Bunce CM (2012) A quick, simple and unbiased method to quantify C2C12 myogenic differentiation. Muscle Nerve 44: 366–370.

33. Bradford MM (1976) Rapid and sensitive method for the quantitation of microgram quantities of protein utilizing the principle of protein-dye binding. Anal Biochem 72: 248–254.

34. Lin HY, Davis FB, Luidens MK, Mousa SA, Cao JH, et al. (2011) Molecular basis for certain neuroprotective effects of thyroid hormone. Front Mol Neurosci 4: 29.

35. Monk JA, Sims NA, Dziegielewska KM, Weiss RE, Ramsay RG, et al. (2013) Delayed development of specific thyroid hormone-regulated events in transthyretin null mice. Am J Physiol Endocrinol Metab. 304: E23–31.

36. Molkentin JD, Olson EN (1996) Defining the regulatory networks for muscle development. Curr Opin Gen Dev 6: 445–453.

37. Gayraud-Morel B, Chrétien F, Flamant P, Gomès D, Zammit PS, et al (2007) A role for the myogenic determination gene Myf5 in adult regenerative myogenesis. Dev Biol 312: 13–28.

38. Darbellay B, Arnaudeau S, König S, Jousset H, Bader C, et al. (2009) STIM1- and Orai1-dependent store-operated calcium entry regulates human myoblast differentiation. 284: 5370–80.

39. Lyfenko AD, Dirksen RT (2008) Differential dependence of store-operated and excitation-coupled Ca2+ entry in skeletal muscle on STIM1 and Orai1. J Physiol 586: 4815–24.

40. Stiber J, Hawkins A, Zhang ZS, Wang S, Burch J, et al. (2008) STIM1 signalling controls store-operated calcium entry required for development and contractile function in skeletal muscle. Nat Cell Biol 10: 688–97.

41. Kotturi MF, Carlow DA, Lee JC, Ziltener HJ, Jefferies WA (2003) Identification and functional characterization of voltage-dependent calcium channels in T lymphocytes. J Biol Chem 278: 46949–60.

42. Kotturi MF, Jefferies WA (2005) Molecular characterization of L-type calcium channel splice variants expressed in human T lymphocytes. Mol Immunol 42: 1461–74.

43. Andrés V, Walsh K (1996) Myogenin expression, cell cycle withdrawal, and phenotypic differentiation are temporally separable events that precede cell fusion upon myogenesis. J Cell Biol 132: 657–66.

44. Cognard C, Constantin B, Rivet-Bastide M, Imbert N, Besse C, et al. (1993) Appearance and evolution of calcium currents and contraction during the early post-fusional stages of rat skeletal muscle cells developing in primary culture. Development 117: 1153–61.

45. Hou X, Parkington HC, Coleman HA, Mechler A, Martin LL, et al. (2007) Transthyretin oligomers induce calcium influx via voltage-gated calcium channels. J Neurochem 100: 446–57.

46. Porter GA, Makuck RF, Rivkees SA (2002) Reduction in intracellular calcium level inhibits myoblast differentiation. J Biol Chem 277: 28942–28947.

47. Liu JH, Bijlenga P, Occhiodoro T, Fischer-Lougheed J, Bader CR, et al. (1999) Mibefradil (Ro 40–5967) inhibits several Ca2+ and K+ currents in human fusion-competent myoblasts. Br J Pharmacol 126: 245–50.

48. Slotkin TA, Seidler FJ, Kavlock RJ, Bartolome JV (1992) Thyroid hormone differentially regulates cellular development in neonatal rat heart and kidney. Teratology 45: 303–12.

49. Hennemann G, Docter R, Friesema EC, de Jong M, Krenning EP, et al. (2001) Plasma Membrane Transport of Thyroid Hormones and Its Role in Thyroid Hormone Metabolism and Bioavailability. Endocrine Reviews 22: 451–476.

50. Carnac G, Albagli-Curiel O, Desclozeaux M, Vandromme M, Glineur C, et al. (1993) Overexpression of c-erbA proto-oncogene enhances myogenic differentiation. Oncogene 8: 3103–10.

51. Rosen HN, Moses AC, Murrell JR, Liepnieks JJ, Benson MD (1993) Thyroxine interactions with transthyretin: a comparison of 10 different naturally occurring human transthyretin variants. J Clin Endocrinol Metab 77: 370–4.

52. Downes M, Griggs R, Atkins A, Olson EN, Muscat GE (1993) Identification of a thyroid hormone response element in the mouse myogenin gene: characterization of the thyroid hormone and retinoid X receptor heterodimeric binding site. Cell Growth Differ 4: 901–9.